Imposing Quasineutrality via the Dirac Theory of Constraints

Philip J. Morrison

Department of Physics, Institute for Fusion Studies,
and ODEN Institute Applied Mathematics Group

The University of Texas at Austin

morrison@physics.utexas.edu https://web2.ph.utexas.edu/∼morrison/

AAPPS26 Busan, Korea

October 12, 2026

Supported by:
The US Department of Energy Office FES #DE-FG02-04ER-54742
The National Science Foundation #2512309

Long History of Quasineutrality

- Magnetofluid models: Langmuir $\rightarrow$ Alfvén, XMHD, ...

- Kinetic Theory $\longleftarrow$

Imposing quasineutrality on electrostatic plasmas via the Dirac theory of constraints

Dimitrios Kaltsas[1,2], Joshua W. Burby[3], Philip J. Morrison[3], Emanuele Tassi[4] and George Throumoulopoulos[1]

[1]Department of Physics, University of Ioannina, Ioannina 451 10, Greece
[2]Department of Informatics, Democritus University of Thrace, Kavala 654 04, Greece
[3]Department of Physics and Institute for Fusion Studies, The University of Texas at Austin, Austin, TX 78712, USA
[4]CNRS, Observatoire de la Côte d'Azur, Laboratoire J. L. Lagrange, Boulevard de l'Observatoire, Université Côte d'Azur, CS 34229, 06304 Nice CEDEX 4, France

Corresponding author: Dimitrios Kaltsas, d.kaltsas@uoi.gr

(Received 7 August 2025; revision received 11 December 2025; accepted 2 January 2026)

We present a method for imposing quasineutrality and, more generally, charge density conservation in the Vlasov–Poisson (VP) and Vlasov–Ampère (VA) systems, which describe electrostatic plasma dynamics, by applying the Dirac theory of constraints. Leveraging the Hamiltonian field formulations of the VP and VA models, we construct generalised Dirac brackets using the Dirac algorithm. The resulting constrained systems enforce charge density conservation, and consequently quasineutrality, given that the initial charge density is zero, through new advection terms in the Vlasov equations involving generalised-force terms, while the electric field is eliminated from the constrained Vlasov dynamics. To verify charge density conservation we conduct one-dimensional numerical experiments using a semi-Lagrangian method, demonstrating that the enforcement of the quasineutrality constraint significantly modifies the dynamics. This approach enables us to identify the forces required to enforce quasineutrality, offering a systematic way to assess the validity of the quasineutral approximation across different kinetic scales.

Key words: plasma dynamics, plasma properties, plasma simulation

General 2-Fluid Theory for species $s \in \{\pm\}$

Momentum : $$m_s n_s \left(\frac{\partial \boldsymbol{v}_s}{\partial t} + \boldsymbol{v}_s \cdot \nabla \boldsymbol{v}_s \right) = -\nabla p_s + \nabla \cdot \Pi_s + e_s n_s \left(\boldsymbol{E} + \boldsymbol{v}_s \times \boldsymbol{B} \right) + \boldsymbol{R}_s$$

Continuity : $$\frac{\partial n_s}{\partial t} = -\nabla \cdot (n_s \boldsymbol{v}_s)$$

Entropy : $$\frac{\partial s_s}{\partial t} + \boldsymbol{v}_s \cdot \nabla s_s = -\frac{1}{n_s m_s T_s} \nabla \cdot Q_s + \frac{1}{n_s m_s T_s} \Pi_s : \nabla \boldsymbol{v}_s$$ (alternatively T_s *or* p_s)

Sources – Charge and Current : $\rho_e = \sum_s e_s n_s$ and $\boldsymbol{J} = \sum_s e_s n_s \boldsymbol{v}_s$

Local Thermo : $U_s(\rho_s, s_s)$ *st* $T_s = \frac{\partial U_s}{\partial s_s}$ and $p_s = \rho_s^2 \frac{\partial U_s}{\partial \rho_s}$

Maxwell : $\epsilon_0 \nabla \cdot \boldsymbol{E} = \rho_e$ and $\epsilon_0 \frac{\partial \boldsymbol{E}}{\partial t} = \frac{1}{\mu_0} \nabla \times \boldsymbol{B} - \boldsymbol{J}$

Stress and collisions : $\Pi_s \sim \sum \eta_s^a \nabla \boldsymbol{v}_s$ and $\sum_s \boldsymbol{R}_s = 0$

Reduction to Extended MHD (e.g. Luest (1959)

Kepler 2-Body:

$$\boldsymbol{R}_{cm} = \frac{m_1 \boldsymbol{r}_1 + m_2 \boldsymbol{r}_2}{m_1 + m_2} \quad \text{and} \quad \boldsymbol{r} = \boldsymbol{r}_1 - \boldsymbol{r}_2$$

Magnetofluid:

$$\boldsymbol{v} = \frac{m_+ n_+ \boldsymbol{v}_+ + m_- n_- \boldsymbol{v}_-}{m_+ n_+ + m_+ n_+} \quad \text{and} \quad \boldsymbol{J} = e(n_+ \boldsymbol{v}_+ - n_- \boldsymbol{v}_-)$$

Coodinate Change:

$$\boxed{\textbf{Extended MHD} \ + \ \textbf{Non} - \textbf{Quasineutrality Terms Isolated}}$$

Neutrality vs. Quasineutrality:

$$\int d^3 r \left(n_+(\boldsymbol{r}, t) - n_-(\boldsymbol{r}, t) \right) = 0 \quad \text{vs.} \quad n_+(\boldsymbol{r}, t) = n_-(\boldsymbol{r}, t) = n(\boldsymbol{r}, t)$$

Extended MHD

Continuity equation:

$$\frac{\partial \rho}{\partial t} = -\nabla \cdot (\rho \boldsymbol{V}), \qquad \rho = m_+ n_+ + m_- n_- = (m_+ + m_-) n$$

Momentum Equation;

$$\rho \left(\frac{\partial \boldsymbol{V}}{\partial t} + (\boldsymbol{V} \cdot \nabla) \boldsymbol{V} \right) = -\nabla p + \boldsymbol{J} \times \boldsymbol{B} - \frac{m_-}{e} (\boldsymbol{J} \cdot \nabla) \frac{\boldsymbol{J}}{en},$$

Faraday's Law:

$$\frac{\partial \boldsymbol{B}}{\partial t} = -\nabla \times \boldsymbol{E}$$

Ohm's Law

$$\boldsymbol{E} = -\boldsymbol{V} \times \boldsymbol{B} + \frac{1}{en} (\boldsymbol{J} \times \boldsymbol{B} - \nabla p_e) + \frac{m_-}{e^2 n} \left[\frac{\partial \boldsymbol{J}}{\partial t} + \nabla \cdot (\boldsymbol{V}\boldsymbol{J} + \boldsymbol{J}\boldsymbol{V}) \right] - \frac{m_-}{e^2 n} (\boldsymbol{J} \cdot \nabla) \frac{\boldsymbol{J}}{en} + \frac{\boldsymbol{J}}{\sigma}$$

$\rightarrow$ **Model reductions** based on asymptotics, small parameter expansions, such as Hall MHD, Inertial MHD, 1960s – 1980s –, reduced MHD, gyrofluid models, Hasegawa-Mima or quasigeostrophy, various reduced fluid models ...

Maxwell-Vlasov

The Vlasov Equation:

$$\frac{\partial f_\alpha}{\partial t} + \mathbf{v} \cdot \nabla_{\mathbf{x}} f_\alpha + \frac{q_\alpha}{m_\alpha} (\mathbf{E} + \mathbf{v} \times \mathbf{B}) \cdot \nabla_{\mathbf{v}} f_\alpha = 0$$

Species α, mass m_α, charge q_α, distribution function $f_\alpha(\mathbf{x}, \mathbf{v}, t)$.

Maxwell's Equations:

$$\nabla \cdot \mathbf{E} = \frac{\rho}{\epsilon_0} \qquad \text{and} \qquad \nabla \cdot \mathbf{B} = 0$$

$$\nabla \times \mathbf{E} = -\frac{\partial \mathbf{B}}{\partial t} \qquad \text{and} \qquad \nabla \times \mathbf{B} = \mu_0 \mathbf{J} + \mu_0 \epsilon_0 \frac{\partial \mathbf{E}}{\partial t}$$

Coupling:

$$\rho(\mathbf{x}, t) = \sum_\alpha q_\alpha \int f_\alpha(\mathbf{x}, \mathbf{v}, t)\, d^3v \quad \text{and} \quad \mathbf{J}(\mathbf{x}, t) = \sum_\alpha q_\alpha \int \mathbf{v} f_\alpha(\mathbf{x}, \mathbf{v}, t)\, d^3v$$

Quasineutrality:

$$\rho(\mathbf{x}, t) = \sum_\alpha q_\alpha \int f_\alpha(\mathbf{x}, \mathbf{v}, t)\, d^3v \approx 0$$

Maintained over time if $\nabla \cdot \mathbf{J} = 0$.

Vlasov-Poisson and Ampere

Vlasov-Poisson:

$$\frac{\partial f_\alpha}{\partial t} + \mathbf{v} \cdot \nabla_{\mathbf{x}} f_\alpha - \frac{q_\alpha}{m_\alpha} \nabla_{\mathbf{x}} \phi \cdot \nabla_{\mathbf{v}} f_\alpha = 0$$

$$-\nabla^2 \phi = \frac{\rho}{\epsilon_0} = \frac{1}{\epsilon_0} \sum_\alpha q_\alpha \int f_\alpha \, d^3 v$$

Quasineutrality:

$$\sum_\alpha q_\alpha n_\alpha(\mathbf{x}, t) = 0$$

Vlasov-Ampère System:

$$\frac{\partial f_\alpha}{\partial t} + \boldsymbol{v} \cdot \nabla_{\mathbf{x}} f_\alpha + \frac{q_\alpha}{m_\alpha} \boldsymbol{E} \cdot \nabla_{\mathbf{v}} f_\alpha = 0$$

$$\frac{\partial \boldsymbol{E}}{\partial t} = -\boldsymbol{J}/\epsilon_0 = -\frac{1}{\epsilon_0} \sum_\alpha q_\alpha \int \boldsymbol{v} f_\alpha \, dv$$

Quasineutrality:

$$\boldsymbol{J}(t) = \sum_\alpha q_\alpha \int \boldsymbol{v} f_\alpha \, dv \,, \qquad \rho = 0, \ \nabla \cdot \mathbf{J} = 0$$

Main Question

- Belief $\lambda_D \to 0 \Rightarrow$ QN is valid. But

What forces would be required to maintain quasineutrality?

- Knowing these forces can serve as a diagnostic. When they are big, QN is probably not a good approximation.

- Any forces? One can restrict to forces that preserve other constraints, energy conservation, Casimir invariants, Hamiltonian structure, ... **Dirac's constraint method.**

- We propose a systematic way to remove fast time (e.g. plasma oscillations) scales in numerics, while preserving structure.

Hamilton's Canonical Equations

Phase Space with Canonical Coordinates: (q, p)

Hamiltonian function: $H(q, p)$ $\leftarrow$ the energy

Equations of Motion:

$$\boxed{\dot{p}_i = -\frac{\partial H}{\partial q^i} \quad \text{and} \quad \dot{q}^i = \frac{\partial H}{\partial p_i}} \qquad i = 1, 2, \ldots N$$

Phase Space Coordinate Rewrite: $z = (q, p)\,, \quad \alpha, \beta = 1, 2, \ldots 2N$

$$\dot{z}^\alpha = J_c^{\alpha\beta} \frac{\partial H}{\partial z^\beta} = \{z^\alpha, H\}_c \quad \text{where} \quad (J_c^{\alpha\beta}) = \begin{pmatrix} 0_N & I_N \\ -I_N & 0_N \end{pmatrix}$$

$J_c :=$ Poisson tensor, Hamiltonian bi-vector, cosymplectic form

Dirac's Method – Simple Canonical Case

Dirac Bracket:

$$\{F,G\}_D = \{F,G\}_c + \frac{\{F,C_1\}_c\{C_2,G\}_c}{\{C_1,C_2\}_c} - \frac{\{F,C_2\}_c\{C_1,G\}_c}{\{C_1,C_2\}_c}$$

Enforces any two constraints C_1 and C_2 if $\{C_1,C_2\}_c \neq 0$.

Creates Casimirs! Preserves the Jacobi identity.

Noncanonical Hamiltonian Structure

Sophus Lie (1890) $\longrightarrow$ PJM (noncanonical 1980) $\longrightarrow$ Weinstein (1982) Poisson Manifolds

Noncanonical Coordinates:

$$\dot{z}^{\alpha} = \{z^{\alpha}, H\} = J^{\alpha\beta}(z)\frac{\partial H}{\partial z^{\beta}}$$

Noncanonical Poisson Bracket:

$$\{f, g\} = \frac{\partial f}{\partial z^{\alpha}} J^{\alpha\beta}(z) \frac{\partial g}{\partial z^{\beta}}$$

Bilinear Poisson Bracket Properties:

antisymmetry $\rightarrow$ $\{f, g\} = -\{g, f\}$ $\rightarrow$ $J^{\alpha\beta} = -J^{\beta\alpha}$

Jacobi identity $\rightarrow \{f, \{g, h\}\} + \{b, \{h, f\}\} + \{h, \{f, g\}\} = 0 \rightarrow$ Jacobiator $S^{\alpha\beta\gamma} = J^{\alpha\ell}\partial_{\ell} J^{\beta\gamma} + cyc \equiv 0$

Leibniz $\rightarrow$ $\{fh, g\} = f\{h, g\} + \{h, g\}f\,, \qquad fg$ pointwise

G. Darboux: $detJ \neq 0 \Longrightarrow J \rightarrow J_c$ Canonical Coordinates

Sophus Lie: $detJ = 0 \Longrightarrow$ Canonical Coordinates plus Casimirs $\leftarrow$ G. Sudarshan
(Lie's distinguished functions!)

Poisson Manifold (phase space) $\mathcal{Z}$ Cartoon

Degeneracy in $J \Rightarrow$ Casimirs:

$$\{f, C\} = 0 \quad \forall\ f : \mathcal{Z} \to \mathbb{R}$$

Lie-Darboux Foliation by Casimir (symplectic) leaves:

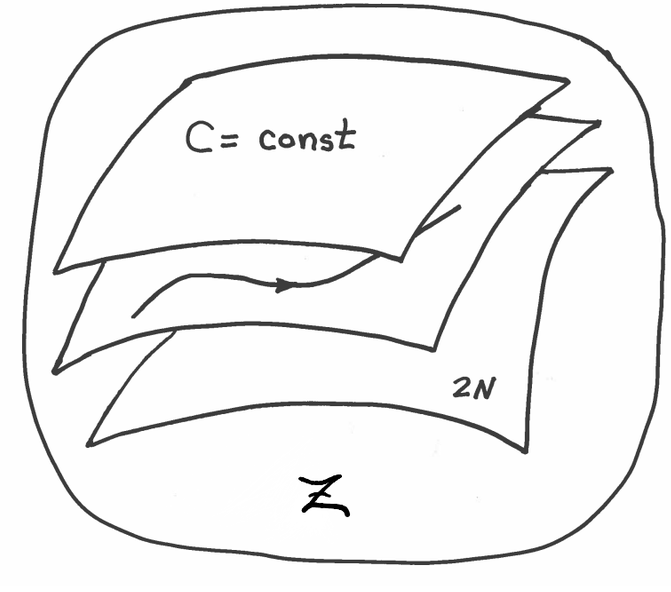

Dirac's Method – Noncanonical Case

Dirac's method works for noncanonical Poisson brackets (pjm, Liebovitz, and Biello (2009)).

Dirac Bracket:

$$\{F,G\}_D = \{F,G\} + \frac{\{F,C_1\}\{C_2,G\}}{\{C_1,C_2\}} - \frac{\{F,C_2\}\{C_1,G\}}{\{C_1,C_2\}}$$

Preserves any two incipient constraints C_1 and C_2.

- Preserves Dirac constraints $C_{1,2}$ **and** any Casimirs of $\{F,G\}$

Used extensively for vortex dynamics in pjm and Flierl, Physica D 240, 212–232 (2011).

Noncanonical Hamiltonian Field Theory

All nondissipative basic plasma theories have Hamiltonian form in terms of noncanonical Poisson brackets.

Noncanonical Poisson Bracket:

$$\{F, G\} = \int d^n x \, \frac{\delta F}{\delta \chi} \mathcal{J} \frac{\delta G}{\delta \chi}$$

F, G = functionals like total energy, χ = fluid variables, $\delta F/\delta \chi$ = functional derivative, and $\mathcal{J}$ = special operator $\Rightarrow$ Poisson bracket properties of Lie algebra realization ....

See pjm, Rev. Mod. Phys. **70**, 467 (1998) to get the basics.

Dirac constraint theory can be used with any of these.

Sample Equations of Motion

Equations of Motion:

$$\partial_t f_s = -\boldsymbol{v}\cdot\nabla f_s - \frac{q_s}{m_s}\boldsymbol{E}\cdot\nabla_{\boldsymbol{v}} f_s \pm \frac{1}{m_s}\Big\{\nabla\alpha\cdot\nabla f_s - [(\boldsymbol{v}\cdot\nabla)\nabla\alpha - \nabla\beta + \nabla\gamma]\cdot\nabla_{\boldsymbol{v}} f_s$$
$$+ q_s\nabla_{\boldsymbol{v}} f_s\cdot\nabla\mathcal{L}^{-1}\nabla\cdot\int d^3v\,\boldsymbol{E}\left(\frac{f_i}{m_i}+\frac{f_e}{m_e}\right)\Big\}, \tag{3.30}$$

where $+$ corresponds to the ion equation and $-$ to the electron equation. In (3.30) the quantities α, β, γ are

$$\alpha = \mathcal{L}^{-1}\nabla\cdot\int d^3v\,\boldsymbol{v}(f_i - f_e) = e^{-1}\mathcal{L}^{-1}\nabla\cdot\boldsymbol{J}, \tag{3.31}$$

$$\beta = \mathcal{L}^{-1}\nabla\cdot[(\boldsymbol{M}\cdot\nabla)\nabla\alpha + \boldsymbol{M}\Delta\alpha + (\nabla\alpha\cdot\nabla)\boldsymbol{M}], \tag{3.32}$$

$$\gamma = \mathcal{L}^{-1}\nabla\cdot\int d^3v\,\boldsymbol{v}\boldsymbol{v}\cdot\nabla(f_i - f_e) = \mathcal{L}^{-1}\nabla\nabla : (\boldsymbol{P}_i - \boldsymbol{P}_e)\,; \tag{3.33}$$

$$\mathcal{L} := \nabla\cdot\left[\left(\frac{n_i}{m_i}+\frac{n_e}{m_e}\right)\right]$$

Computations 1D 2 Spieces Plasma

Perturbed counterstreaming (nonsymmetric) beam equilibria for both species.

Electron-Proton and Electron -Positron

Use semi-lagrangian (Cheng-Knorr) 2 species, remove fast time.

We verify

- The numerical algorithmic satisfies the constraints on the charge-density distribution and current incompressibility.
- The QN dynamics deviates from standard VP dynamics – with identical initial conditions.

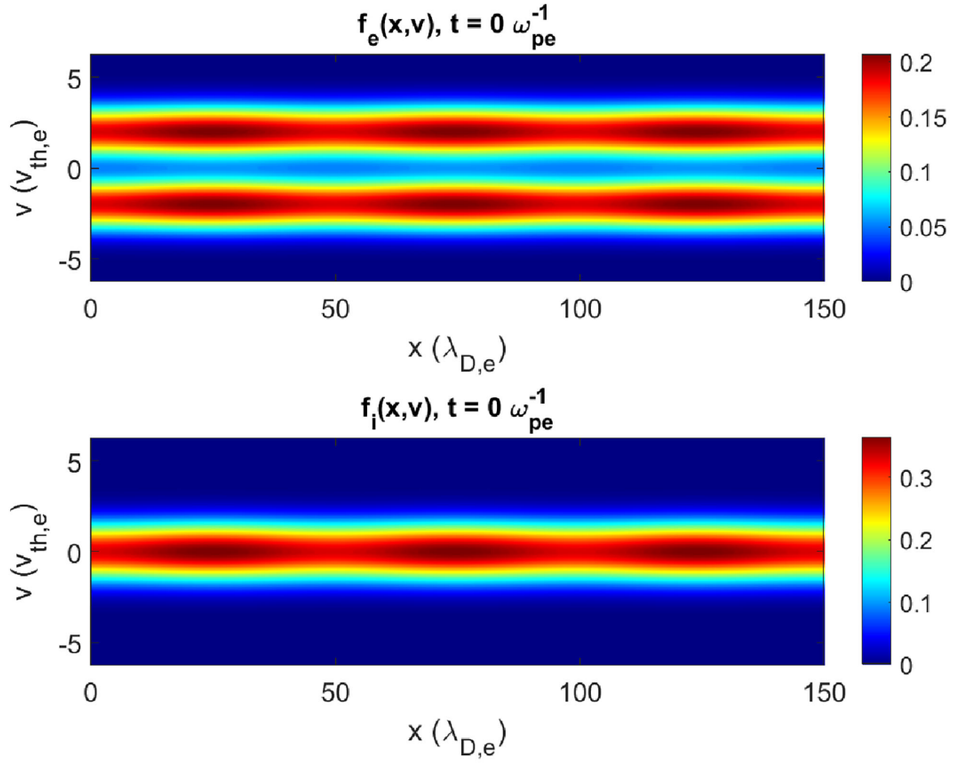

FIGURE 1. Initial conditions of the distribution functions f_e and f_i in phase space. The electron distribution forms two separated beams since V_e is large enough in (4.21), whereas the two ion beams are so close to each other that they effectively form a single beam with zero macroscopic velocity. This broad, centralised ion beam was found to favour numerical stability over longer simulation times.

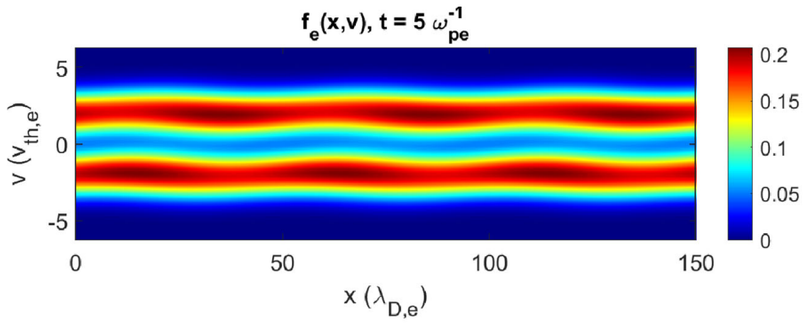
$f_e(x,v)$, t = 5 ω_{pe}^{-1}
v ($v_{th,e}$)
x ($\lambda_{D,e}$)
5
0
-5
0
50
100
150
0.2
0.15
0.1
0.05
0

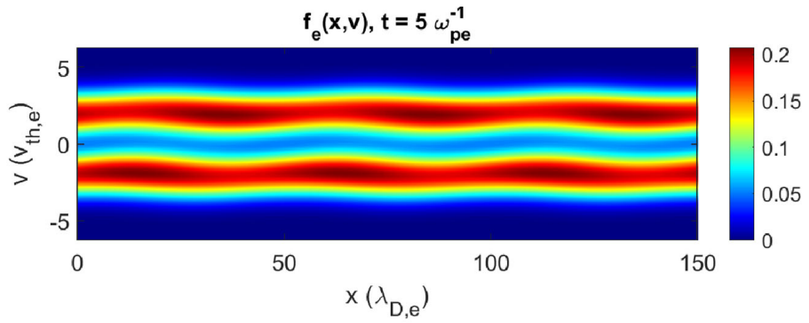
$f_e(x,v)$, t = 5 ω_{pe}^{-1}
v ($v_{th,e}$)
x ($\lambda_{D,e}$)
5
0
-5
0
50
100
150
0.2
0.15
0.1
0.05
0

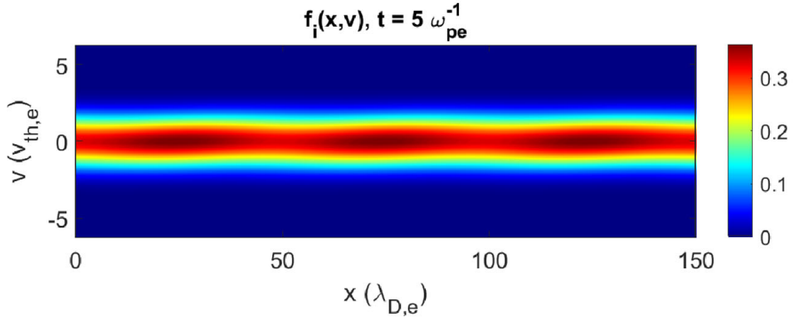
$f_i(x,v)$, t = 5 ω_{pe}^{-1}
v ($v_{th,e}$)
x ($\lambda_{D,e}$)
5
0
-5
0
50
100
150
0.3
0.2
0.1
0

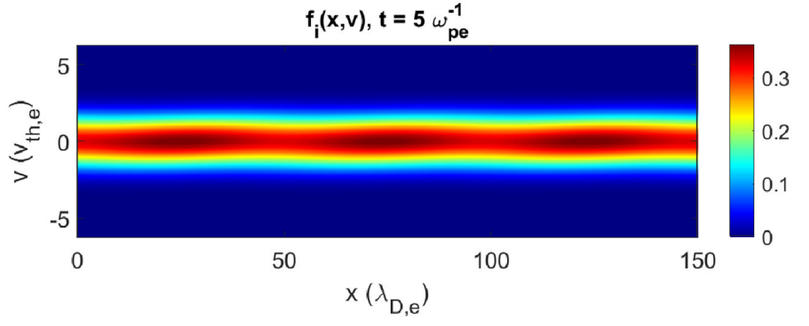
$f_i(x,v)$, t = 5 ω_{pe}^{-1}
v ($v_{th,e}$)
x ($\lambda_{D,e}$)
5
0
-5
0
50
100
150
0.3
0.2
0.1
0

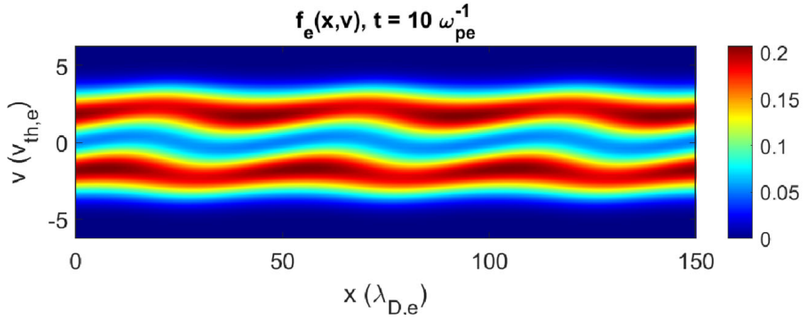
$f_e(x,v)$, t = 10 ω_{pe}^{-1}
v ($v_{th,e}$)
x ($\lambda_{D.e}$)
5
0
-5
0
50
100
150
0.2
0.15
0.1
0.05
0

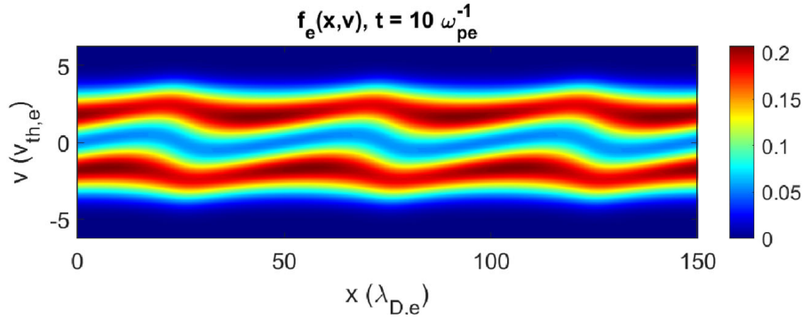
$f_e(x,v)$, t = 10 ω_{pe}^{-1}
v ($v_{th,e}$)
x ($\lambda_{D.e}$)
5
0
-5
0
50
100
150
0.2
0.15
0.1
0.05
0

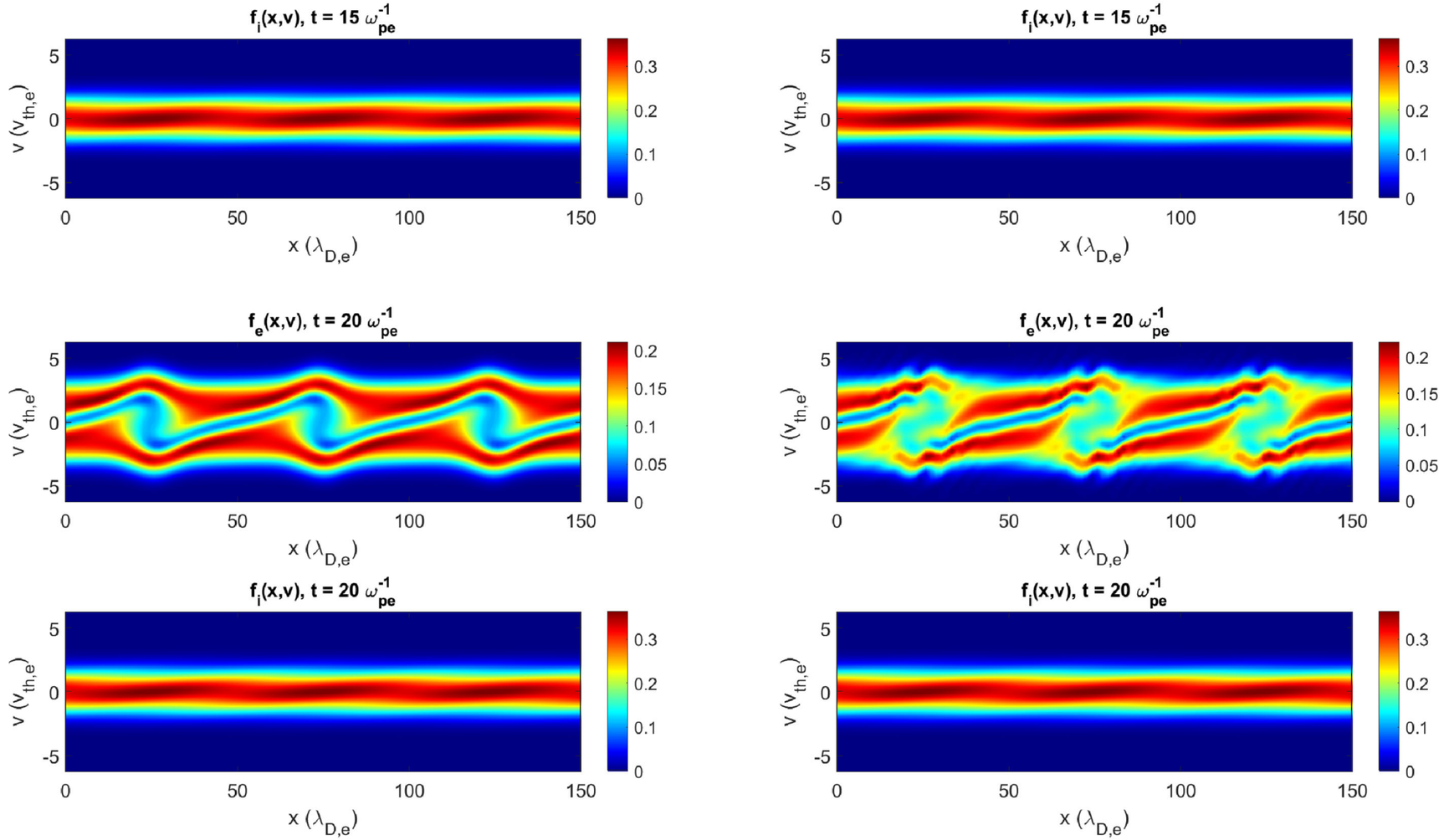

FIGURE 2. Snapshots of the electron and ion distribution functions in phase space (x, v) at different times. The left-hand column corresponds to the VP case and the right-hand column to the QN case. A distinct evolution of f_e is observed between the two scenarios, especially during the nonlinear phase.

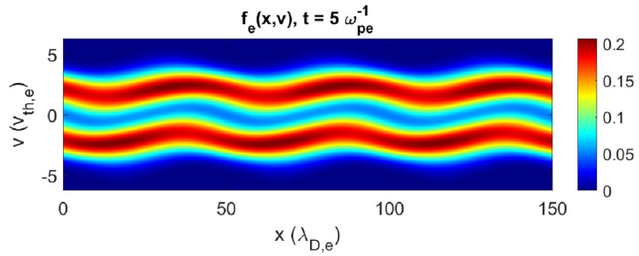
$f_e(x,v)$, t = 5 ω_{pe}^{-1}
v ($v_{th,e}$)
x ($\lambda_{D,e}$)
0.2
0.15
0.1
0.05
0

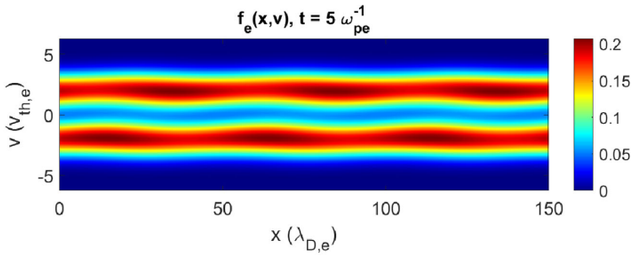
$f_e(x,v)$, t = 5 ω_{pe}^{-1}
v ($v_{th,e}$)
x ($\lambda_{D,e}$)
0.2
0.15
0.1
0.05
0

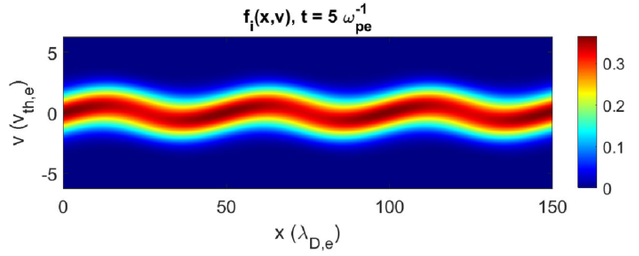
$f_i(x,v)$, t = 5 ω_{pe}^{-1}
v ($v_{th,e}$)
x ($\lambda_{D,e}$)
0.3
0.2
0.1
0
5
0
-5
0
50
100
150

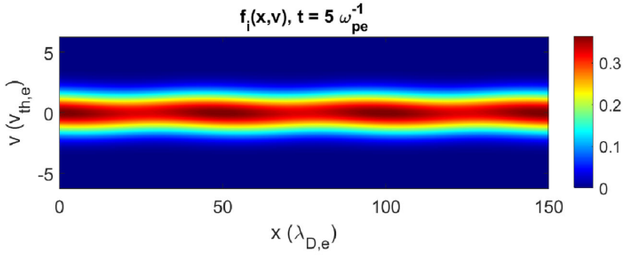
$f_i(x,v)$, t = 5 ω_{pe}^{-1}
v ($v_{th,e}$)
x ($\lambda_{D,e}$)
0.3
0.2
0.1
0
5
0
-5
0
50
100
150

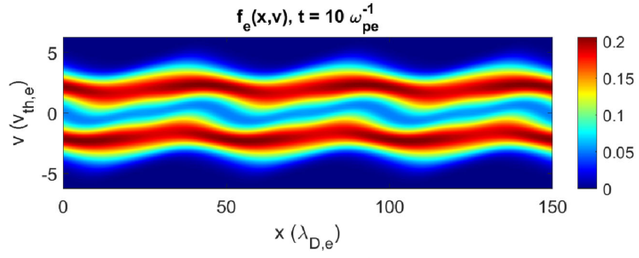
$f_e(x,v)$, t = 10 ω_{pe}^{-1}
v ($v_{th,e}$)
x ($\lambda_{D,e}$)
0.2
0.15
0.1
0.05
0

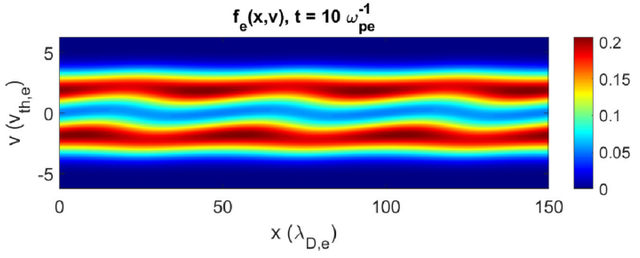
$f_e(x,v)$, t = 10 ω_{pe}^{-1}
v ($v_{th,e}$)
x ($\lambda_{D,e}$)
0.2
0.15
0.1
0.05
0

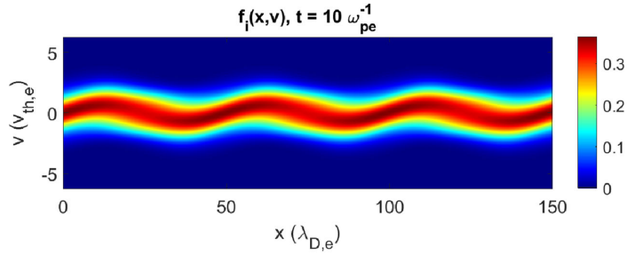
$f_i(x,v)$, t = 10 ω_{pe}^{-1}
v ($v_{th,e}$)
x ($\lambda_{D,e}$)
0.3
0.2
0.1
0
5
0
-5
0
50
100
150

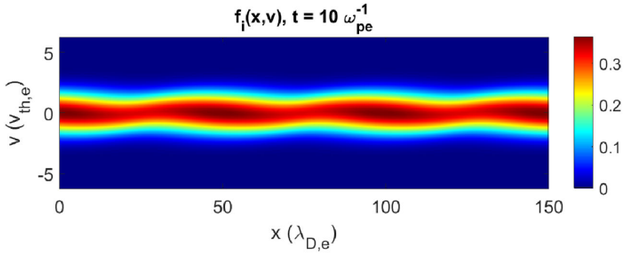
$f_i(x,v)$, t = 10 ω_{pe}^{-1}
v ($v_{th,e}$)
x ($\lambda_{D,e}$)
0.3
0.2
0.1
0
5
0
-5
0
50
100
150

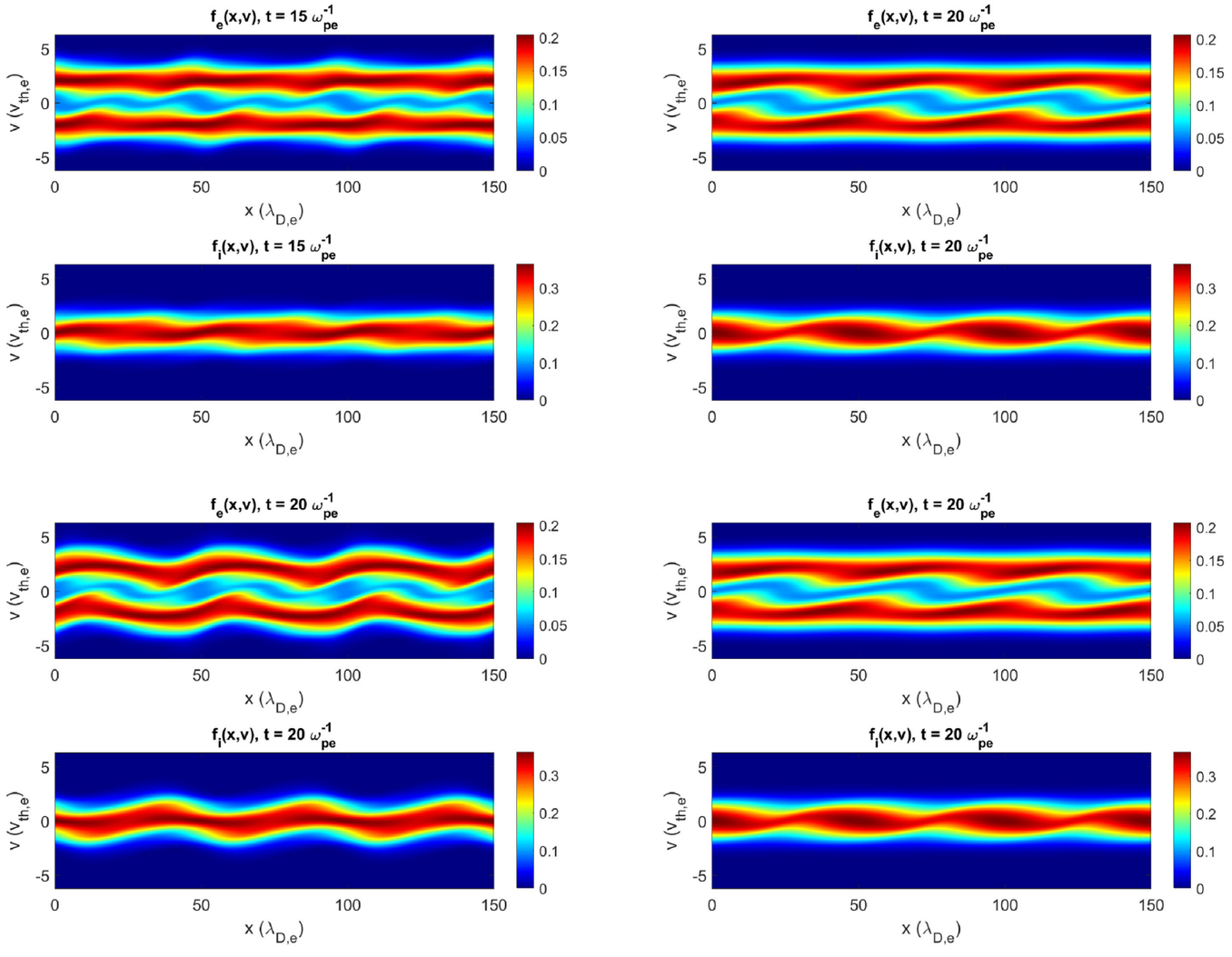

FIGURE 6. Snapshots of the electron and positron distribution functions in phase space (x, v) at different times. The left column corresponds to the VP case and the right column to the QN case. We observe distinct evolution for both f_e and f_i.

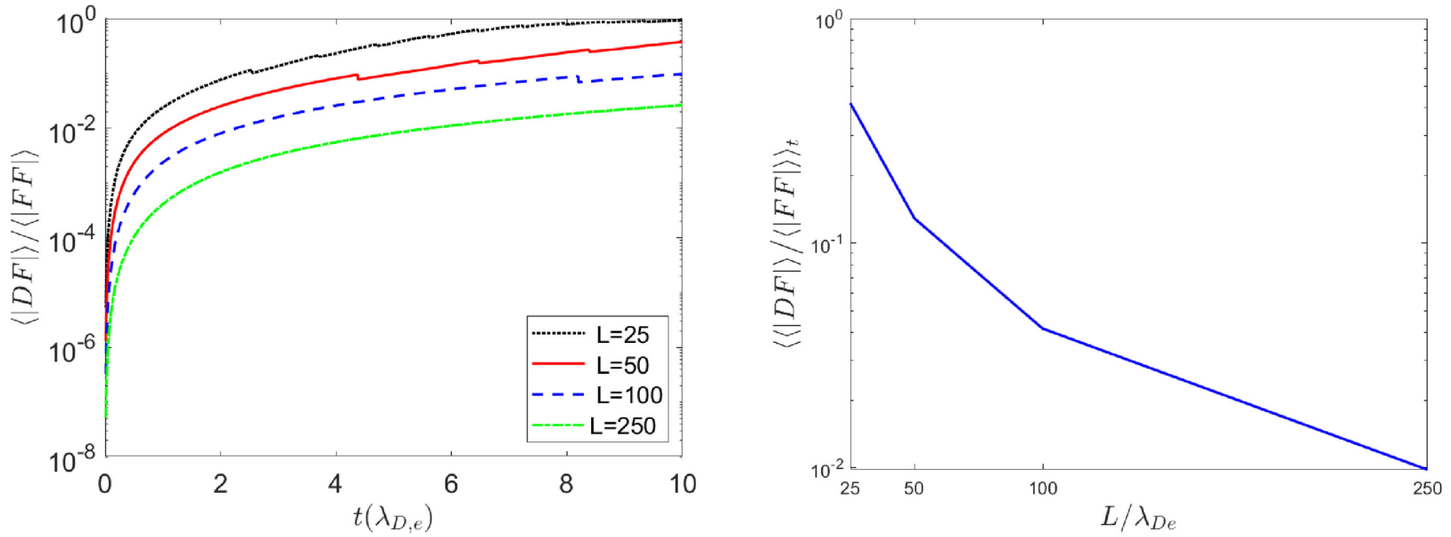

FIGURE 8. Left: The evolution of the ratio (4.27) of the Dirac forces over the fluid forces for a simulation with steady ion distribution. In all four cases $L = 25$, $L = 50$, $L = 100$ and $L = 250$, this ratio increases with time and becomes progressively smaller for larger length scales. Right: The time-averaged ratio versus the length scale L.